



A Census of the Most Luminous Stars. I. The Upper HR Diagram for the Large Magellanic Cloud

John C. Martin¹ and Roberta M. Humphreys²

¹University of Illinois Springfield, USA; jmart5@uis.edu

²Minnesota Institute for Astrophysics, University of Minnesota, USA

Received 2023 July 31; revised 2023 October 4; accepted 2023 October 5; published 2023 October 30

Abstract

Spectral classification and multiwavelength photometry for the most luminous stars in the LMC has greatly increased due to several recent surveys for both the hottest and coolest members. Combining data from these spectroscopic and photometric surveys, we have created catalogs based on their spectral classifications of the different groups: the luminous O and B stars, the A-type supergiants, and the evolved yellow and red supergiants. We derive their stellar parameters based on spectroscopic characteristics, and discuss the problems with extinction in crowded fields and the role of binarity on selected stars. Based on these surveys, we present the upper HR diagram representative of the LMC massive star population greater than $20 M_{\odot}$.

Unified Astronomy Thesaurus concepts: Massive stars (732); Large Magellanic Cloud (903)

Supporting material: machine-readable tables

1. Introduction

The most luminous and massive stars and the final stages in their evolution are critical for our understanding of supernovae and the subsequent enrichment of the interstellar medium, the formation of neutron stars and black holes, and the “first stars.” The upper HR diagram is complicated. Stars with the same luminosity and temperature can have very different mass loss histories and evolutionary states. Mass loss including nonterminal giant eruptions can determine their final fate. The relationships among various groups of evolved and mass losing stars such as luminous blue variables (LBVs), B[e] supergiants, Wolf Rayet stars, and the hypergiants requires an enhanced census of the upper HR diagram. Unfortunately, the initial mass function limits the number of very massive stars, so that studies of individual star clusters yield small samples in only the youngest clusters. In our own galaxy the sample is also incomplete, limited by interstellar extinction and uncertainty in distances over the full extent of the Galactic disk even with the advantages of Gaia.

Alternatively, star-forming galaxies in the Local Group provide more complete samples of luminous star populations with all the stars essentially at the same distance. Recent photometric surveys (Massey 2002; Zaritsky et al. 2004; Evans et al. 2011) and GAIA DR3 (Gaia Collaboration et al. 2023) have established rich photometric database for the Large Magellanic Cloud (LMC). But HR diagrams for the LMC constructed from photometry alone cannot always differentiate foreground stars from members of the LMC and recognize emission line stars. They can also exclude stars with exceptional extinction or other properties. Selecting stars by spectral type combined with multiwavelength photometry ensures more accurate identification and determination of effective temperature and extinction for individual targets. Also, many past surveys have excluded the Tarantula nebula due to extreme crowding and high/uncertain extinction but now the VTFS

survey (Evans et al. 2011) addresses many of those limitations so those stars can be included in a full census of the LMC.

In this study, we combine photometric and spectroscopic surveys of the LMC to produce a *spectroscopically-selected* HR diagram of stars more massive than $20 M_{\odot}$. By relying on spectral identification and focusing on the most luminous stars (brighter than $\log(L_{\odot}) > 4.7$), significant foreground contamination should be limited in all but the coolest and latest spectral types. In the next two sections we describe the selection of the OBA-type stars, and discuss the yellow supergiants (YSGs) and red supergiants (RSGs). The extinction and luminosity are determined for each star relying on the spectral type and recent calibrations. The effects of strong spectral emission, crowding and binarity are also considered. The HR diagram is presented and discussed in the final section.

2. OBA-type Star Selection

Stars of spectral type A8 and earlier were selected based on the classifications of Ardeberg et al. (1972), Brunet et al. (1975), Walborn (1977), Rousseau et al. (1978), Crampton (1979), Conti et al. (1986), Fitzpatrick (1988), Parker & Garmany (1993), Massey et al. (1995, 2000), and Jaxon et al. (2001). Early large-scale spectral surveys were favored for their accuracy and uniformity. Several of them required careful curation because they are not available in machine-readable form with accurate positions. Additional stars were selected from the VLT-FLAMES Tarantula Survey (Walborn et al. 2014) and by crossmatching Zaritsky et al. (2004)³ with spectral types in SIMBAD (Wenger et al. 2000).⁴ Special classes of hot luminous stars (i.e., luminous blue variables and B[e] supergiants) are *excluded from the catalog*.

Johnson UBV photometry was obtained primarily from Massey (2002), Brunet et al. (1975), Rousseau et al. (1978), Conti et al. (1986), Parker & Garmany (1993), or Evans et al. (2011). In the absence of photometry from those sources Zaritsky et al. (2004) was used (see Appendix). When there



Original content from this work may be used under the terms of the [Creative Commons Attribution 4.0 licence](#). Any further distribution of this work must maintain attribution to the author(s) and the title of the work, journal citation and DOI.

³ In Appendix we discuss the development of a necessary correction to the *U*-band photometry in the Zaritsky et al. (2004) catalog.

⁴ Sources cited by SIMBAD are given in Table 12.

Table 1
Adopted Values by Spectral Type

| Sp. Type | (B-V) ₀ | Log(T_{eff}) | B.C (mags) | Sp. Type | Log(T_{eff}) | B.C (mags) |
|-----------------|--------------------|-------------------------|------------|------------|-------------------------|------------|
| Supergiants (I) | | | | | | |
| O3 | -0.33 | 4.626 | -3.87 | O3 | 4.647 | -4.03 |
| O4 | -0.33 | 4.607 | -3.74 | O4 | 4.628 | -3.88 |
| O5 | -0.32 | 4.587 | -3.61 | O5 | 4.605 | -3.73 |
| O6 | -0.31 | 4.566 | -3.46 | O6 | 4.582 | -3.57 |
| O7 | -0.29 | 4.544 | -3.31 | O7 | 4.557 | -3.40 |
| O8 | -0.29 | 4.521 | -3.16 | O8 | 4.531 | -3.23 |
| O9 | -0.28 | 4.496 | -2.99 | O9 | 4.503 | -3.04 |
| O9.5 | -0.27 | 4.484 | -2.91 | O9.5 | 4.488 | -2.94 |
| O9.7 | -0.26 | 4.469 | -2.82 | O9.7 | 4.452 | -2.73 |
| B0 | -0.25 | 4.454 | -2.74 | B0 | 4.418 | -2.52 |
| B0.2 | -0.23 | 4.427 | -2.58 | B0.2 | 4.386 | -2.34 |
| B0.5 | -0.21 | 4.377 | -2.29 | B0.5 | 4.356 | -2.18 |
| B0.7 | -0.20 | 4.331 | -2.05 | B0.7 | 4.328 | -2.03 |
| B1 | -0.18 | 4.309 | -1.93 | B1 | 4.301 | -1.89 |
| B1.5 | -0.17 | 4.287 | -1.82 | B1.5 | 4.275 | -1.76 |
| B2 | -0.16 | 4.247 | -1.62 | B2 | 4.229 | -1.53 |
| B2.5 | -0.14 | 4.228 | -1.52 | B2.5 | 4.208 | -1.41 |
| B3 | -0.12 | 4.209 | -1.42 | B3 | 4.188 | -1.31 |
| B4 | -0.11 | 4.174 | -1.23 | | | |
| B5 | -0.08 | 4.127 | -0.96 | Dwarfs (V) | | |
| B6 | -0.06 | 4.100 | -0.80 | | | |
| B7 | -0.05 | 4.071 | -0.64 | O3 | 4.652 | -4.05 |
| B8 | -0.03 | 4.040 | -0.46 | O4 | 4.632 | -3.91 |
| B9 | -0.02 | 4.013 | -0.31 | O5 | 4.611 | -3.77 |
| B9.5 | 0.00 | 3.992 | -0.21 | O6 | 4.590 | -3.62 |
| A0 | 0.02 | 3.978 | -0.15 | O7 | 4.567 | -3.47 |
| A2 | 0.05 | 3.965 | -0.10 | O8 | 4.543 | -3.03 |
| A5 | 0.10 | 3.929 | 0.00 | O9 | 4.517 | -3.13 |
| A8 | 0.14 | 3.913 | 0.02 | O9.5 | 4.504 | -3.04 |
| F0 | 0.16 | 3.895 | 0.03 | O9.7 | 4.488 | -2.97 |
| F2 | 0.20 | 3.874 | 0.03 | B0 | 4.452 | -2.73 |
| F5 | 0.26 | 3.845 | 0.03 | B0.2 | 4.418 | -2.52 |
| F8 | 0.37 | 3.813 | 0.01 | B0.5 | 4.386 | -2.34 |
| G0 | 0.55 | 3.778 | -0.04 | B0.7 | 4.356 | -2.18 |
| G2 | 0.63 | 3.764 | -0.07 | B1 | 4.328 | -2.03 |
| G5 | 0.76 | 3.741 | -0.14 | B1.5 | 4.301 | -1.89 |
| G8 | 0.98 | 3.700 | -0.30 | B2 | 4.275 | -1.76 |
| K0 | 1.12 | 3.663 | -0.53 | | | |
| K5 | 1.57 | 3.585 | -1.09 | | | |
| M0 | 1.61 | 3.573 | -1.31 | | | |
| M1 | 1.63 | 3.568 | -1.45 | | | |
| M2 | 1.65 | 3.559 | -1.69 | | | |
| M3 | 1.67 | 3.549 | -2.01 | | | |
| M4 | 1.70 | 3.538 | -2.18 | | | |
| M5 | 1.70 | 3.538 | -2.49 | | | |

Table 2
Average Extinction of O-Type Stars in LMC Clusters

| R.A.J2000 | Decl.J2000 | Radius (arcmin) | N stars ^a | Avg A_V | Comments |
|-----------|------------|-----------------|----------------------|-----------|-------------------------------|
| 84.64157 | -69.11476 | 3.5 | 75 | 1.222 | NGC 2070 (Tarantula Nebula) |
| 84.43089 | -69.16632 | 1.5 | 17 | 1.366 | Extended Tarantula Nebula |
| 84.75127 | -69.49901 | 2.0 | 14 | 1.138 | NGC 2074 |
| 82.70307 | -71.06600 | 3.0 | 12 | 0.605 | [GKK2003] O236 (open cluster) |
| 80.53637 | -67.93357 | 3.0 | 23 | 0.675 | LH 47 |
| 81.44631 | -67.49502 | 2.5 | 3 | 1.171 | L54S,L51S, O236 |
| 83.09506 | -66.46582 | 2.5 | 3 | 0.166 | MHK 1041 (star cluster) |
| 83.88639 | -66.03622 | 3.0 | 6 | 0.393 | NGC 2030 |
| 74.17531 | -66.48343 | 2.0 | 19 | 0.409 | NGC 1761 |

Note.

^a Number of O-type stars in cluster with $A_V > 0$, excluding known and suspected binaries.

Table 3
O-type Supergiants

| R.A. J2000 | decl. J2000 | Name | V | (B-V) | (U-B) | Phot Source ^a | Sp Type | Sp Type Source ^a | A _V | A _V Flag ^b | Log(T _{eff}) | M _{Bol} |
|------------|-------------|-------------------------|-------|-------|-------|--------------------------|----------|-----------------------------|----------------|----------------------------------|------------------------|------------------|
| 71.86501 | -70.56268 | SK -70 1a | 13.65 | -0.05 | -0.90 | R78 | O9II | C86 | 0.71 | 0 | 4.50 | -8.58 |
| 72.46671 | -67.68750 | SK -67 4 | 13.02 | -0.16 | -0.98 | R78 | O9Ib | J01 | 0.37 | 0 | 4.50 | -8.84 |
| 72.90995 | -69.49827 | IRSF J04513837-6929542 | 13.87 | -0.14 | -1.16 | Z04 | O3.5O6If | M14 | 0.58 | 0 | 4.62 | -9.02 |
| 72.94129 | -69.34064 | 2MASS J04514589-6920261 | 13.34 | -0.14 | -1.01 | Z04 | O9.7Ib | SIM | 0.37 | 0 | 4.47 | -8.35 |
| 72.94566 | -69.31794 | CTIO85 23 | 13.16 | 0.17 | -0.91 | Z04 | O9.7Ib | SIM | 1.33 | 0 | 4.47 | -9.49 |

3

Notes.^a See Table 12 for key to abbreviations.^b Extinction is: 0 = estimated from spectral type, 1 = average value across LMC, 2 = average value from stars in same region (for O-type stars)

(This table is available in its entirety in machine-readable form.)

Table 4
B-type Supergiants

| R.A. J2000 | decl. J2000 | Name | V | (B–V) | (U–B) | Phot Source ^a | SpType | SpType Source ^a | A_V | A_V Flag ^b | $\log(T_{\text{eff}})$ | M_{bol} |
|------------|-------------|---------|-------|-------|-------|--------------------------|--------|----------------------------|-------|-------------------------|------------------------|------------------|
| 70.15500 | −68.29427 | SOI 297 | 13.92 | 0.07 | −0.46 | Z04 | B9Ib | SIM | 0.28 | 0 | 4.01 | −5.17 |
| 70.67763 | −68.35182 | ARDB 2 | 13.60 | −0.03 | −0.42 | R78 | B8:I: | S72 | 0.00 | 0 | 4.04 | −5.36 |
| 71.04928 | −69.30209 | SOI 447 | 13.78 | 0.00 | −0.42 | A72 | B7Ib | SIM | 0.16 | 0 | 4.07 | −5.52 |
| 71.11896 | −69.67617 | SOI 449 | 13.51 | 0.06 | −0.18 | A72 | B8Ib | SIM | 0.29 | 0 | 4.04 | −5.74 |
| 71.18682 | −69.29464 | SOI 451 | 13.98 | 0.06 | −0.46 | Z04 | B9Ib | SIM | 0.27 | 0 | 4.01 | −5.10 |

Notes.^a See Table 12 for key to abbreviations.^b Extinction is: 0 = estimated from spectral type, 1 = average value across LMC, 2 = average value from stars in same region (for O-type stars).

(This table is available in its entirety in machine-readable form.)

Table 5
A-type Supergiants

| R.A. J2000 | decl. J2000 | Name | V | (B–V) | (U–B) | Phot Source ^a | SpType | SpType Source ^a | A_V | A_V Flag ^b | $\log(T_{\text{eff}})$ | M_{bol} |
|------------|-------------|-----------|-------|-------|-------|--------------------------|--------|----------------------------|-------|-------------------------|------------------------|------------------|
| 70.77955 | −70.45868 | SOI 696 | 13.09 | 0.21 | ... | H15 | A3I | R78 | 0.46 | 0 | 3.95 | −5.93 |
| 71.59925 | −69.86503 | SOI 456 | 13.80 | 0.36 | 14.22 | Z04 | A5Ib | SIM | 0.84 | 0 | 3.93 | −5.54 |
| 71.76841 | −68.65186 | SOI 299 | 13.92 | 0.06 | 14.12 | R78 | A7:I | R78 | 0.22 | 1 | 3.92 | −4.79 |
| 71.80518 | −69.69462 | SOI 459 | 13.45 | 0.13 | ... | H15 | A5I | R78 | 0.09 | 0 | 3.93 | −5.14 |
| 71.88854 | −69.24250 | HD 268612 | 12.47 | 0.23 | 12.90 | A72 | A2I | A72 | 0.58 | 0 | 3.96 | −6.71 |

Notes.^a See Table 12 for key to abbreviations.^b Extinction is: 0 = estimated from spectral type, 1 = average value across LMC, 2 = average value from stars in same region (for O-type stars).

(This table is available in its entirety in machine-readable form.)

was insufficient data or the photometry yielded a nonsensical color excess (likely to occur in crowded fields), other measurements were found in: Ardeberg et al. (1972), Isserstedt (1979), Isserstedt (1982), Fitzpatrick (1988), Parker (1992), Schild & Testor (1992), Parker et al. (1992), Parker (1993), Malumuth & Heap (1994), Oey & Massey (1995), Oey (1996a), Will et al. (1997), Massey et al. (2005), Evans et al. (2006), Bonanos et al. (2009), or De Marchi et al. (2011).

The selection of stars with spectral types OBA was magnitude limited to focus on masses greater than $20 M_{\odot}$, roughly corresponding to $M_{\text{bol}} < −7.0$. Assuming a distance modulus to the LMC of 18.5 (Wagner-Kaiser et al. 2017) and an average extinction of $A_V \sim 1.0$, this corresponds to O-type stars brighter than $V < 16.5$ (for a B.C. range of ~ -4 to -3), B-type stars brighter than $V < 15.5$ (for B.C. ~ -3 to -1), and A-type stars brighter than $V < 14.5$ (for B.C. ~ -1 to 0).

Table 1 includes the adopted intrinsic colors, T_{eff} , and bolometric corrections for spectral types from O3 to M5 based on recent calibrations for O stars from Martins et al. (2005), for B- and A-type supergiants from Flower (1996) and for the cooler stars (Section 3) from Flower (1996) and Levesque et al. (2006). In cases where the star had no luminosity class, it was assigned using the spectral type, photometry, and tables of Humphreys & McElroy (1984).

Absolute visual magnitudes (M_V) were determined in the usual way using $E(B-V)$, $R = 3.2$ and a distance modulus of 18.5 for the LMC. When available, the absolute visual magnitudes published in the VLT-FLAMES Tarantula survey (Evans et al. 2011) were adopted. Extra scrutiny was given to stars with negative $E(B-V)$. OB-type stars with negative color excess occurred predominantly in compact star-forming regions. Negative $E(B-V)$ can be a result of strong emission which is common in early type supergiants. When they could not be otherwise resolved, negative $E(B-V)$ values for OB stars

were replaced by the median $E(B-V)$ value from other stars of the same type in the same star-forming region (see Table 2). A-type stars with negative $E(B-V)$ that could not be resolved with better photometry are removed.

An anomalous luminosity is often caused by the influence of a known or undetected binary companion or other unresolved blend. Most work to determine the binary frequency for hot luminous stars has focused on O-type stars. Mason et al. (2009), Barbá et al. (2010) and more recent surveys (see Sana (2017) Table 1) have found that between 50% and 60% of the O-type stars in the Milky Way are binary. A similar binary fraction has been observed for O-type stars in the Tarantula region of the LMC (Sana et al. 2013; Almeida et al. 2017). The binary fraction of B-type stars is lower (20%–40%), especially among supergiants evolved off the main sequence (Dunstall et al. 2015; Banyard et al. 2022; Guo et al. 2022).

Both SIMBAD (Wenger et al. 2000) and Dunstall et al. (2015) were used to identify known and suspected binaries or unresolved blends (Table 6). 30% of the O stars and 8.5% of the B-type stars in our samples are known or suspected binaries or blends. Only one of the A-type stars is a known binary. It is very likely we have not identified all the binaries in our sample. Five stars ([FBM2009] 41, MCPS 085.10302-69.67033, PGW 3073, SK -69 25, and MCPS 084.86883-69.45283) are flagged as suspected blends for being unrealistically luminous for their spectral types. Since anomalous luminosities can also be a result of foreground contamination, stars were checked for Gaia DR3 parallaxes (Gaia Collaboration et al. 2022) with greater than three sigma significance, proper motions, and radial velocities consistent with LMC membership.

Tables 3, 4, and 5 show the format for the separate catalogs for the O-, B-, and A-type supergiants. The full lists of 635 O-type, 2034 B-type, and 339 A-type supergiants are available

Table 6
OBA-type Known and Suspected Binaries

| R.A. J2000 | decl. J2000 | Name | V | (B-V) | (U-B) | Phot Source ^a | Binary Class ^c | SpType | SpType Source ^a | A _V | A _V Flag ^b | Log(T _{eff}) | M _{Bol} |
|------------|-------------|-------------------|-------|-------|-------|--------------------------|---------------------------|----------|----------------------------|----------------|----------------------------------|------------------------|------------------|
| 72.46422 | -69.20119 | SK -69 9 | 12.56 | -0.15 | -0.96 | R78 | EB | B0: | R78 | 0.32 | 0 | 4.45 | -9.00 |
| 72.46432 | -69.20107 | SK -69 9 | 12.54 | -0.13 | -0.77 | B09 | EB | O6.6III | J01 | 0.52 | 0 | 4.57 | -9.97 |
| 73.08029 | -69.34704 | OGLE LMC-ECL-1886 | 14.31 | -0.08 | -0.72 | M02 | EB | O9.5V: | SIM | 0.59 | 0 | 4.50 | -7.82 |
| 73.25367 | -68.02569 | BI 12 | 13.48 | -0.18 | -1.04 | B75 | EB | O7.5III | SIM | 0.33 | 0 | 4.54 | -8.67 |
| 73.35605 | -70.59436 | SK -70 10 | 13.28 | -0.15 | -0.10 | R78 | EB | B0III[e] | R12a | 0.32 | 0 | 4.45 | -8.27 |

5

Notes.^a See Table 12 for key to abbreviations for sources of photometry and spectral types.^b 0 = estimated from spectral type, 1 = average value across LMC, 2 = average value from stars in same region (for O-type stars)^c Multiplicity types: blend = unresolved blend of more than one star, EB = eclipsing binary, SB = Spectroscopic Binary, HMXB = high mass x-ray binary, and ? = suspected or uncertain.

(This table is available in its entirety in machine-readable form.)

Table 7
Yellow Supergiants

| R.A. J2000 | decl. J2000 | Name | <i>J</i> ^b | <i>H</i> ^b | <i>K_s</i> ^b | <i>V</i> | (B–V) | Phot Source ^a | SpType | SpType Source ^a | <i>A_V</i> | Log(<i>T_{eff}</i>) | <i>M_{Bol}</i> |
|------------|-------------|----------------|-----------------------|-----------------------|-----------------------------------|----------|-------|--------------------------|--------|----------------------------|----------------------|-------------------------------|------------------------|
| 72.30833 | −68.96992 | SOI 465 | 11.45 | 11.24 | 11.16 | 12.48 | 0.43 | M02 | F5 I | R78 | 0.42 | 3.85 | −6.7 |
| 72.73271 | −69.43128 | HD 268687 | 9.69 | 9.45 | 9.36 | 10.65 | 0.47 | A72 | F6 Ia | A72 | 0.54 | 3.83 | −8.5 |
| 73.08000 | −69.07847 | HD 268708 | 10.64 | 10.48 | 10.36 | 11.60 | 0.35 | A72 | F0 I | A72 | 0.61 | 3.90 | −7.6 |
| 73.40496 | −69.71864 | TYC 9165-851-1 | 11.86 | 11.72 | 11.65 | 12.66 | 0.27 | M02 | F2 I | R78 | 0.22 | 3.87 | −6.2 |
| 73.55938 | −69.21019 | HD 268757 R59 | 8.02 | 7.64 | 7.45 | 10.09 | 1.55 | A72 | G8 0 | K76 | 1.76 | 3.70 | −9.6 |

Notes.^a See Table 12 for key to abbreviations.^b From 2MASS point source catalog (Cutri et al. 2003).

(This table is available in its entirety in machine-readable form.)

Table 8
Probable Blended Red Supergiants

| R.A. J2000 | decl. J2000 | Name | <i>J</i> ^b | <i>H</i> ^b | <i>K_s</i> ^b | <i>V</i> | (B–V) | Phot Source ^a | SpType | SpType Source ^a | Log(<i>T_{eff}</i>) | Blend Flag ^c |
|------------|-------------|----------------------|-----------------------|-----------------------|-----------------------------------|----------|-------|--------------------------|--------|----------------------------|-------------------------------|-------------------------|
| 72.54041 | −70.06949 | RM 1-8 | 10.27 | 11.21 | 10.46 | 13.89 | 1.56 | M02 | M: | R83 | 3.57 | 2 |
| 73.14858 | −70.67853 | SP77 32-1 | 9.71 | 8.83 | 8.59 | 12.95 | 1.20 | M02 | M0.5 | W81 | 3.58 | 1 |
| 73.32708 | −69.28431 | LHA 120-S 70 | 9.52 | 8.67 | 8.36 | 12.88 | 1.20 | M02 | M1 | W81 | 3.57 | 2 |
| 73.37850 | −69.29717 | WOH S 60 | 9.32 | 8.46 | 8.06 | 13.00 | 1.03 | M02 | M3 | H90 | 3.56 | 2 |
| 73.66067 | −69.18817 | AP J04543854-6911170 | 8.54 | 7.66 | 7.20 | 13.19 | 1.82 | M02 | M0.5 | W81 | 3.58 | 1 |

Notes.^a See Table 12 for key to abbreviations.^b From 2MASS point source catalog (Cutri et al. 2003).^c Binarityblend was: 1 = confirmed by spectroscopy, 2 = inferred from negative color excess.

(This table is available in its entirety in machine-readable form.)

online. A separate Table 6 is included with the 464 known and suspected OBA-type binaries.

3. YSG and RSG Selection

The selection of the YSGs is outlined in Humphreys et al. (2023). Due to the high foreground contamination in this color range, only YSG with confirmed spectral types F0 to early K and velocities supporting membership in the LMC were selected. Parallaxes and proper motions from the GAIA DR3 catalog (Gaia Collaboration et al. 2022) were used to confirm membership. Spectral types combined with visual and near-infrared photometry were used to derive the visual extinction (A_V) and visual luminosities. Bolometric luminosities were derived from *K*-band photometry following the method of Neugent et al. (2012) using the color excess derived for each individual star. See Humphreys et al. (2023) for details. Table 7 shows the format for the YSG catalog. The full list of 85 stars are available online.

Systematic surveys to determine the binary fraction of supergiants have focused entirely on the hottest (OB) and coolest (RSG) supergiants. Very little is known about the expected binary fraction for yellow supergiants except what may be inferred from their evolutionary status relative to OB supergiants and RSG. We checked the YSG in our list for blends/binarity using SIMBAD. HV 883 (a spectroscopic binary) is the only YSG in our list with any known binary/blend status.

RSGs with spectral types K5 and later, and luminosity classes I, Ia, and Ib were selected from the merged lists of Neugent et al. (2020) and Massey & Olsen (2003). Two

luminous heavily dust obscured RSG identified in Elias et al. (1986) are also included. Like the YSGs, the RSGs are prone to foreground M-giant or M-dwarf contamination. Gaia DR3 (Gaia Collaboration et al. 2022) parallaxes, proper motions, and radial velocities were used to confirm membership in the LMC. Stars were assigned spectral types primarily from Humphreys (1979) and Massey & Olsen (2003). Additional spectral types are from: Cannon (1925), Ardeberg et al. (1972), Hyland et al. (1978), Sanduleak & Philip (1977), Blanco et al. (1980), Westerlund et al. (1981), Rebeirot et al. (1983), Wood et al. (1983), Reid & Mould (1985), Mould & Reid (1987), Lundgren (1988), Reid et al. (1990), Frogel & Blanco (1990), Heydari-Malayeri et al. (1990), and González-Fernández et al. (2015). For ambiguous spectral types (i.e., K5–M3 from Sanduleak & Philip 1977; or M from Rousseau et al. 1978), a mean spectral type or M0 was adopted.

The Johnson BVR photometry is from Massey (2002), Oestreich et al. (1997), or Zaritsky et al. (2004), and the near-infrared JHK magnitudes are from the 2MASS point source catalog (Cutri et al. 2003). Like the OBA-type stars, the E(B–V) color excess for each star was calculated using intrinsic colors in Table 1. Absolute *V* magnitude (M_V) was calculated from the color excess using $R = 3.2$ and assuming a distance modulus of 18.5 for the LMC.

Also like the OBA stars, the RSG selection is magnitude limited to focus on masses greater than $20 M_{\odot}$ roughly corresponding to $M_{\text{bol}} < -7.0$. Assuming an LMC distance modulus of 18.5, average extinction $A_V \sim 1.0$ and bolometric correction between B.C. ~ -1 to -3 this corresponds to $V < 15.5$. This significantly limits contamination by LMC

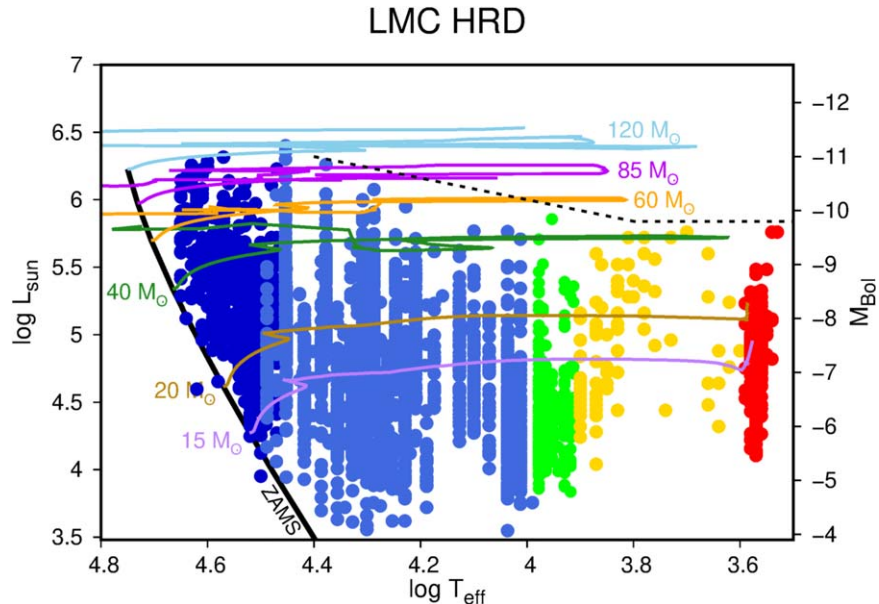


Figure 1. The Hertzsprung–Russell diagram for the most luminous and massive stars in the Large Magellanic Cloud. The Zero Aged Main Sequence (ZAMS) is noted with a solid black line. The Humphreys/Davidson limit (Humphreys & Davidson 1979) is noted with the dashed black line. Stars are colored as follows: O-type = dark blue, B-type = light blue, A-type = green, YSG = yellow, RSG = red. The ZAMS and evolutionary tracks are adopted from Eggenberger et al. (2021) $Z = 0.006$ nonrotating models (LMC is $Z = 0.004$).

Table 9
Red Supergiants

| R.A. J2000 | decl. J2000 | Name | J^b | H^b | K_s^b | V | (B–V) | Phot Source ^a | SpType | SpType Source ^a | A_V | Log(T_{eff}) | M_{Bol} |
|------------|-------------|------------|-------|-------|---------|-------|-------|--------------------------|--------|----------------------------|-------|-------------------------|------------------|
| 72.36154 | -68.75167 | SP77 22-10 | 9.42 | 8.50 | 8.12 | 13.30 | 1.94 | M02 | M1 | W81 | 0.99 | 3.57 | -7.69 |
| 72.45701 | -69.92601 | RM 1-7 | 10.09 | 9.26 | 8.98 | 13.54 | 1.69 | M02 | M: | R83 | 0.26 | 3.57 | -6.75 |
| 72.74454 | -69.23411 | SP77 31-5 | 9.43 | 8.60 | 8.36 | 12.88 | 1.95 | M02 | M0 | W81 | 1.09 | 3.58 | -7.54 |
| 72.83807 | -68.94768 | RM 1-14 | 10.29 | 9.38 | 9.09 | 13.99 | 1.96 | M02 | M: | R83 | 1.12 | 3.57 | -6.74 |
| 72.87913 | -69.24778 | SP77 31-6 | 9.43 | 8.55 | 8.24 | 13.55 | 1.94 | M02 | M0.5 | W81 | 1.02 | 3.58 | -7.64 |

Notes.

^a See Table 12 for key to abbreviations.

^b From 2MASS point source catalog (Cutri et al. 2003).

(This table is available in its entirety in machine-readable form.)

AGB or super-AGB stars. Stars without luminosity class are included if they met the limiting magnitude criteria.

Binary companions to RSG should be bluer than RSG and almost all RSG binaries should have either O or B star companions (Neugent et al. 2018, 2019). Therefore stars with observed colors bluer than the intrinsic colors for an RSG are probably blends. Suspected blends, with negative color excess ($E(B-V) < 0$) are listed in Table 8 along with binary RSG noted by composite spectral type and/or spectroscopically confirmed by Neugent et al. (2020). The number of RSG in our list which are confirmed or suspected blends ($\sim 20\%$) is consistent with the estimates of binary frequency by Neugent et al. (2020) and Patrick et al. (2019). Table 8 shows the format for the catalogs of blended RSG. The full list of 61 blended RSG is available online.

Bolometric corrections were computed following the method of Neugent et al. (2012) with differences in how the color excess and effective temperature were determined. Neugent et al. (2012) assumed a constant color excess of $E(B-V) = 0.13$ for all LMC stars. The average color excess for RSG in our sample is significantly greater (for single RSG, $E(B-V)_{\text{avg}} = 0.27$). So we adopted the $E(B-V)$ computed individually for each star from spectral type and intrinsic

colors. Neugent et al. (2012) calculated effective temperatures from (J–K) colors. Instead we used effective temperatures derived from the spectral types (Table 1). For two luminous heavily dust obscured RSG identified in Elias et al. (1986; WOH G 64 and IRAS 05346-6949), T_{eff} and M_{Bol} were directly adopted from that publication. Table 9 shows the format for the RSG catalog. The full list 244 RSG is available online.

4. The Upper HR Diagram

The HR diagram for the most luminous and most massive stars in the LMC, from our spectroscopy-based survey and resulting catalogs is shown in Figure 1. The most luminous stars of each type in our catalog are listed in Table 10.

We have not tried to evaluate the completeness of the catalog. Since we relied on spectroscopic surveys to identify the stars, the completeness of those respective surveys will determine the relative completeness of the different classes of stars by spectral type. Instead we show the luminosity functions for the OB-type stars (Figure 2), the two spectroscopic groups that are most likely to be main sequence stars. We set out to produce a catalog of stars in the LMC with masses greater than $20 M_{\odot}$ corresponding roughly to $\log(L_{\odot}) > 4.7$ and the catalog

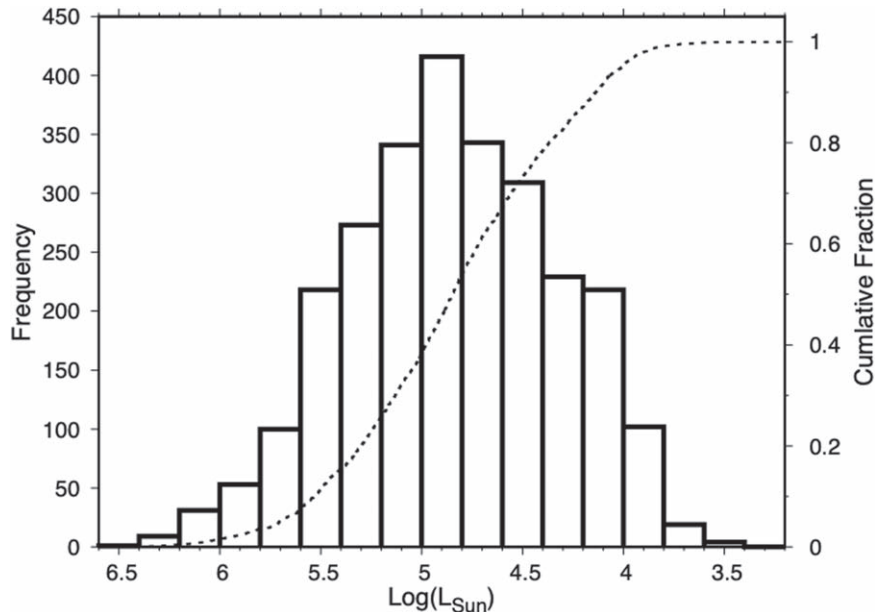


Figure 2. The luminosity distribution for O and B-type stars in the catalog (frequency read off the left axis). The cumulative fraction going toward lower luminosity is read off the right hand axis.

Table 10
Most Luminous LMC Supergiants of Each Spectral Type

| Name | SpType | M_{Bol} |
|---|------------------|------------------|
| O-type supergiants (O3-O9) $M_{\text{Bol}} \leq -10.80$ | | |
| 2MASS J04542610-6911022 | O7V | -10.99 |
| W61 3-20 | O5-6V((f))z | -10.91 |
| CPD-69 471 | O2I _f | -10.84 |
| PGMW 3120 | O5.5V((f*)) | -10.80 |
| Early B-type supergiants (B0-B1) $M_{\text{Bol}} \leq -11.00$ | | |
| HD 37836 | B0e | -11.81 |
| HD 269327 | B0: | -11.20 |
| HD 268804 | OB0 | -11.09 |
| Mid B-type supergiants (B2-B5) $M_{\text{Bol}} \leq -9.40$ | | |
| HD 269649 | B2.5: | -10.07 |
| HD 269992 | B2Ia | -9.55 |
| HD 269997 | B3Ia | -9.48 |
| LHA 120-S 46 | B2 | -9.47 |
| Late B-type supergiants (B6-B9) $M_{\text{Bol}} \leq -9.40$ | | |
| HD 269923 | B6I | -9.62 |
| HD 268851 | B8 | -9.61 |
| HD 32034 | B9Iae | -9.47 |
| A-type supergiants (A0-A8) $M_{\text{Bol}} \leq -9.00$ | | |
| HD 33579 | A3Ia | -9.84 |
| HD 33579 | A3IaO | -9.84 |
| HD 269902 | A0I | -9.47 |
| HD 270086 | A1IaO | -9.01 |
| Yellow supergiants (F0-K4) $M_{\text{Bol}} \leq -9.50$ | | |
| HD 268757 R59 | G8Ia | -9.6 |
| HD 271182 R92 | F8Ia | -9.5 |
| HD 269723 | G4Ia | -9.5 |
| HD 269953 | G0Ia | -9.5 |
| Red supergiants (K5-M4) $M_{\text{Bol}} \leq -8.80$ | | |
| WOH G 64 | M5 | -9.60 |

Table 10
(Continued)

| Name | SpType | M_{Bol} |
|-----------------|--------|------------------|
| IRAS 05346-6949 | M5 | -9.60 |
| /W60/ A27 | M1Ia | -8.91 |
| SV* HV 888 | M4Ia | -8.91 |
| SV* HV 5618 | M1I | -8.82 |

appears to be well populated for masses greater than $15 M_{\odot}$ and $\text{Log}(L_{\odot}) > 4.5$.

The A-type supergiants, YSGs, and RSGs are all post-main-sequence. Several may even be in a post-RSG state. In a recent paper (Humphreys et al. 2023), we identified six high-luminosity yellow supergiants with circumstellar dust as potential post-red supergiants. Similarly, the two most luminous RSGs are highly obscured dusty stars. The RSGs will be discussed in more detail in a forthcoming paper. This enhanced census of the upper HR diagram in the LMC will also be the reference population for a study of special subsets of evolved massive stars such as LBVs and B[e] supergiants to evaluate their associated populations and evolutionary state.

Acknowledgments

We thank the anonymous referee for their constructive comments and we thank the scientific editor for their time facilitating the review.

This study is supported by the University of Illinois Springfield Henry R. Barber Astronomy Endowment funded by the people of Central Illinois.

This research has made use of the SIMBAD database, operated at CDS, Strasbourg, France, and data from the European Space Agency (ESA) mission Gaia (<https://www.cosmos.esa.int/gaia>), processed by the Gaia Data Processing and Analysis Consortium (DPAC; <https://www.cosmos.esa.int/web/gaia/dpac/consortium>). Funding for the DPAC has

been provided by national institutions, in particular the institutions participating in the Gaia Multilateral Agreement.

Appendix

Supplemental Correction to *U*-band Photometry in Zaritsky Catalog

Zaritsky et al. (2004) identified a systematic difference between their *U*-band photometry and Massey (2002). Massey (2002) is better calibrated. Their photometry is preferred, but it does not cover the full spatial extent of the LMC. Zaritsky et al. (2004) replaced photometry in their catalog with data from Massey (2002) for stars which they identified as common between the two catalogs (flagged 1, 11, or 21 in Zaritsky et al. 2004) and suggested a *U*-band correction for the remaining stars.

A spatial crossmatch with a radius of 0''.5 rejecting matches with $dU_{\text{mag}} > 1.0$ mag identified more than 10,000 stars in both Zaritsky et al. (2004) and Massey (2002), which did *not* have their photometry replaced in the Zaritsky et al. (2004) catalog. A plot of those stars revealed a remaining offset between the *U*-band photometry in each catalog *after* applying the Zaritsky et al. (2004) correction. Those data were used to formulate an additional correction (Table 11). Both the Zaritsky et al. (2004) correction and our supplemental correction were applied to the *U*-band photometry of our targets.

Table 12 contains the codes used to reference the photometry and spectroscopy sources.

Table 11
Supplemental Correction to Zaritsky et al. (2004) *U*-band Photometry

| Condition | Supplemental Correction |
|-------------------|--------------------------|
| $U < 13$ | $du_2 = -0.083 U + 1.07$ |
| $13 < U < 14.5$ | $du_2 = -0.020$ |
| $14.5 < U < 15.2$ | $du_2 = -0.038 U + 0.53$ |
| $U > 15.2$ | $du_2 = 0.038 U - 0.62$ |

Table 12
Key for Sources of Photometry and Spectral Types

| Abbreviation | Citation |
|--------------|----------------------------|
| A72 | Ardeberg et al. (1972) |
| B09 | Bonanos et al. (2009) |
| B09 | Bonanos et al. (2009) |
| B17 | Bagnulo et al. (2017) |
| B73 | Brunet et al. (1973) |
| B75 | Brunet et al. (1975) |
| B80 | Blanco et al. (1980) |
| B85 | Bohm-Vitense et al. (1985) |
| B99 | Bosch et al. (1999) |
| C01 | Cidale et al. (2001) |
| C09 | Chen et al. (2009) |
| C78 | Cowley & Hutchings (1978) |
| C79 | Crampton (1979) |
| C86 | Conti et al. (1986) |
| C93 | Cannon & Pickering (1924) |
| C98 | Caloi & Cassatella (1998) |
| D05 | de Wit et al. (2005) |
| D11 | De Marchi et al. (2011) |
| D12 | Dunstall et al. (2012) |
| D18 | Davies et al. (2018) |
| D92a | Deharveng & Caplan (1992) |
| D92b | Deharveng et al. (1992) |

Table 12
(Continued)

| Abbreviation | Citation |
|--------------|----------------------------------|
| E06 | Evans et al. (2006) |
| E10 | Evans et al. (2010) |
| E15a | Evans et al. (2015b) |
| E15b | Evans et al. (2015a) |
| E86 | Elias et al. (1986) |
| F09 | Fariaña et al. (2009) |
| F60 | Feast et al. (1960) |
| F74 | Feast (1974) |
| F87 | Fitzpatrick (1987) |
| F88 | Fitzpatrick (1988) |
| F90 | Frogel & Blanco (1990) |
| F91 | Fitzpatrick (1991) |
| G11a | Gvaramadze & Gualandris (2011) |
| G11b | Girard et al. (2011) |
| G12 | Gvaramadze et al. (2012) |
| G14 | Gvaramadze et al. (2014) |
| G15 | González-Fernández et al. (2015) |
| G87 | Garmann & Walborn (1987) |
| G93 | Gochermann et al. (1993) |
| G94 | Garmann et al. (1994) |
| H00 | Høg et al. (2000) |
| H01 | Heydari-Malayeri et al. (2001) |
| H12 | Hénault-Brunet et al. (2012) |
| H13 | Howarth (2013) |
| H15 | Henden et al. (2015) |
| H74 | Humphreys (1974) |
| H78 | Hyland et al. (1978) |
| H79 | Humphreys (1979) |
| H90 | Heydari-Malayeri et al. (1990) |
| I79 | Isserstedt (1979) |
| I75 | Isserstedt (1975) |
| I82 | Isserstedt (1982) |
| J01 | Jaxon et al. (2001) |
| K12 | Kavanagh et al. (2012) |
| K76 | Keenan & McNeil (1976) |
| L03 | Le Borgne et al. (2003) |
| L88 | Lundgren (1988) |
| M00 | Massey et al. (2000) |
| M02 | Massey (2002) |
| M03 | Massey & Olsen (2003) |
| M05a | Massey et al. (2005) |
| M05b | Meynadier et al. (2005) |
| M06 | Martayan et al. (2006) |
| M12 | Massey et al. (2012) |
| M14 | Massey et al. (2014) |
| M15a | Massey et al. (2015) |
| M15b | McEvoy et al. (2015) |
| M19 | McLeod et al. (2019) |
| M72 | Martin & Rebeiro (1972) |
| M85 | Melnick (1985) |
| M87 | Mould & Reid (1987) |
| M92 | Morgan et al. (1992) |
| M94 | Malumuth & Heap (1994) |
| M95 | Massey et al. (1995) |
| N12 | Neugent et al. (2012) |
| N18 | Neugent et al. (2018) |
| N19 | Neugent et al. (2019) |
| O95 | Oey & Massey (1995) |
| O96a | Oey (1996a) |
| O96b | Oey (1996b) |
| O97 | Oestreicher et al. (1997) |
| P01 | Parker et al. (2001) |
| P12 | Paul et al. (2012) |
| P92a | Parker (1992) |

Table 12
(Continued)

| Abbreviation | Citation |
|--------------|---|
| P92b | Parker et al. (1992) |
| P93a | Parker & Garmany (1993) |
| P93b | Parker (1993) |
| R12a | Reid & Parker (2012) |
| R12b | Rivero González et al. (2012) |
| R13 | Ridley et al. (2013) |
| R18 | Ramachandran et al. (2018) |
| R78 | Rousseau et al. (1978) |
| R85 | Reid & Mould (1985) |
| R83 | Rebeiro et al. (1983) |
| R90 | Reid et al. (1990) |
| S11 | Shanti Priya et al. (2011) |
| S12 | Selier & Heydari-Malayeri (2012) |
| S70 | Sanduleak (1970) |
| S72 | Sanduleak (1972) |
| S76 | Stock et al. (1976) |
| S77 | Sanduleak & Philip (1977) |
| S84 | Shore & Sanduleak (1984) |
| S92 | Schild & Testor (1992) |
| S99a | Smith Neubig & Bruhwiler (1999) |
| S99b | Schmidt-Kaler et al. (1999) |
| SIM | From SIMBAD with no source ^a |
| T82 | Thompson et al. (1982) |
| T98 | Testor & Niemela (1998) |
| V18 | van Jaarsveld et al. (2018) |
| VTFS | Evans et al. (2011) |
| W02a | Walborn et al. (2002a) |
| W02b | Walborn et al. (2002b) |
| W10a | Walborn et al. (2010) |
| W10b | Weidner & Vink (2010) |
| W14 | Walborn et al. (2014) |
| W77 | Walborn (1977) |
| W81 | Westerlund et al. (1981) |
| W83 | Wood et al. (1983) |
| W97a | Will et al. (1997) |
| W97b | Walborn & Blades (1997) |
| Z04 | Zaritsky et al. (2004) |
| Z12 | Zacharias et al. (2012) |
| Z13 | Zastrow et al. (2013) |
| Z86 | Zickgraf et al. (1986) |

Note.

^a This is the classification given in SIMBAD which Wenger et al. (2000) identify as either from Houk & Cowley (1975) or Jaschek (1978).

ORCID iDs

John C. Martin  <https://orcid.org/0000-0002-0245-508X>
Roberta M. Humphreys  <https://orcid.org/0000-0003-1720-9807>

References

- Almeida, L. A., Sana, H., Taylor, W., et al. 2017, *A&A*, 598, A84
 Ardeberg, A., Brunet, J. P., Maurice, E., & Prevot, L. 1972, *A&AS*, 6, 249
 Baglioni, S., Nazé, Y., Howarth, I. D., et al. 2017, *A&A*, 601, A136
 Banyard, G., Sana, H., Mahy, L., et al. 2022, *A&A*, 658, A69
 Barbá, R. H., Gamen, R., Arias, J. I., et al. 2010, RMxAC, 38, 30
 Blanco, V. M., McCarthy, M. F., & Blanco, B. M. 1980, *ApJ*, 242, 938
 Bohm-Vitense, E., Hodge, P., & Proffitt, C. 1985, *ApJ*, 292, 130
 Bonanos, A. Z., Massa, D. L., Sewilo, M., et al. 2009, *AJ*, 138, 1003
 Bosch, G., Terlevich, R., Melnick, J., & Selman, F. 1999, *A&AS*, 137, 21
 Brunet, J. P., Imbert, M., Martin, N., et al. 1975, *A&AS*, 21, 109
 Brunet, J. P., Prevot, L., Maurice, E., & Muratorio, G. 1973, *A&AS*, 9, 447
 Caloi, V., & Cassatella, A. 1998, *A&A*, 330, 492
 Cannon, A. J. 1925, *AnHar*, 100, 17
 Cannon, A. J., & Pickering, E. C. 1924, Henry Draper (HD) Catalog and HD Extension (Cambridge, MA: Harvard College Astronomical Observatory)
 Chen, C. H. R., Chu, Y.-H., Gruendl, R. A., Gordon, K. D., & Heitsch, F. 2009, *ApJ*, 695, 511
 Cidale, L., Zorec, J., & Tringaniello, L. 2001, *A&A*, 368, 160
 Conti, P. S., Garmany, C. D., & Massey, P. 1986, *AJ*, 92, 48
 Cowley, A. P., & Hutchings, J. B. 1978, *PASP*, 90, 636
 Crampton, D. 1979, *ApJ*, 230, 717
 Cutri, R. M., Skrutskie, M. F., van Dyk, S., et al. 2003, VizieR Online Data Catalog, II/246
 Davies, B., Crowther, P. A., & Beasor, E. R. 2018, *MNRAS*, 478, 3138
 De Marchi, G., Paresce, F., Panagia, N., et al. 2011, *ApJ*, 739, 27
 de Wit, W. J., Beaulieu, J. P., Lamers, H. J. G. L. M., Coutures, C., & Meeus, G. 2005, *A&A*, 432, 619
 Deharveng, L., & Caplan, J. 1992, *A&A*, 259, 480
 Deharveng, L., Caplan, J., & Lombard, J. 1992, *A&AS*, 94, 359
 Dunstall, P. R., Dufton, P. L., Sana, H., et al. 2015, *A&A*, 580, A93
 Dunstall, P. R., Fraser, M., Clark, J. S., et al. 2012, *A&A*, 542, A50
 Eggenberger, P., Ekström, S., Georgy, C., et al. 2021, *A&A*, 652, A137
 Elias, J. H., Frogel, J. A., & Schwering, P. B. W. 1986, *ApJ*, 302, 675
 Evans, C. J., Kennedy, M. B., Dufton, P. L., et al. 2015a, *A&A*, 574, A13
 Evans, C. J., Lennon, D. J., Smartt, S. J., & Trundle, C. 2006, *A&A*, 456, 623
 Evans, C. J., Taylor, W. D., Hénault-Brunet, V., et al. 2011, *A&A*, 530, A108
 Evans, C. J., van Loon, J. T., Hainich, R., & Bailey, M. 2015b, *A&A*, 584, A5
 Evans, C. J., Walborn, N. R., Crowther, P. A., et al. 2010, *ApJL*, 715, L74
 Farina, C., Bosch, G. L., Morrell, N. I., Barbá, R. H., & Walborn, N. R. 2009, *AJ*, 138, 510
 Feast, M. W. 1974, *MNRAS*, 169, 273
 Feast, M. W., Thackeray, A. D., & Wesselink, A. J. 1960, *MNRAS*, 121, 337
 Fitzpatrick, E. L. 1987, *ApJ*, 312, 596
 Fitzpatrick, E. L. 1988, *ApJ*, 335, 703
 Fitzpatrick, E. L. 1991, *PASP*, 103, 1123
 Flower, P. J. 1996, *ApJ*, 469, 355
 Frogel, J. A., & Blanco, V. M. 1990, *ApJ*, 365, 168
 Gaia Collaboration, Vallenari, A., Brown, A. G. A., et al. 2023, *A&A*, 674, A1
 Garmany, C. D., Massey, P., & Parker, J. W. 1994, *AJ*, 108, 1256
 Garmany, C. D., & Walborn, N. R. 1987, *PASP*, 99, 240
 Girard, T. M., van Altena, W. F., Zacharias, N., et al. 2011, *AJ*, 142, 15
 Gohermann, J., Grothues, H. G., Oestreich, M. O., Berghoefer, T., & Schmidt-Kaler, T. 1993, *A&AS*, 99, 591
 González-Fernández, C., Dorda, R., Negueruela, I., & Marco, A. 2015, *A&A*, 578, A3
 Guo, Y., Li, J., Xiong, J., et al. 2022, *RAA*, 22, 025009
 Gvaramadze, V. V., Chené, A. N., Kniazev, A. Y., et al. 2014, *MNRAS*, 442, 929
 Gvaramadze, V. V., Chené, A. N., Kniazev, A. Y., & Schnurr, O. 2012, in ASP Conf. Ser. 465, Proc. Scientific Meeting in Honor of Anthony, ed. L. Drissen et al. (San Francisco, CA: ASP), 511
 Gvaramadze, V. V., & Gualandris, A. 2011, *MNRAS*, 410, 304
 Hénault-Brunet, V., Evans, C. J., Sana, H., et al. 2012, *A&A*, 546, A73
 Henden, A. A., Levine, S., Terrell, D., & Welch, D. L. 2015, AAS Meeting Abstracts, 225, 336.16
 Heydari-Malayeri, M., Charmandaris, V., Deharveng, L., et al. 2001, *A&A*, 372, 495
 Heydari-Malayeri, M., Melnick, J., & van Drom, E. 1990, *A&A*, 236, L21
 Høg, E., Fabricius, C., Makarov, V. V., et al. 2000, *A&A*, 355, L27
 Houk, N., & Cowley, A. P. 1975, University of Michigan Catalogue of Two-dimensional Spectral Types for the HD Stars, Vol. I, Declinations -90° to -53°f0 (Ann Arbor, MI: Univ. Michigan)
 Howarth, I. D. 2013, *A&A*, 555, A141
 Humphreys, R. M. 1974, *ApJL*, 190, L133
 Humphreys, R. M. 1979, *ApJS*, 39, 389
 Humphreys, R. M., & Davidson, K. 1979, *ApJ*, 232, 409
 Humphreys, R. M., Jones, T. J., & Martin, J. C. 2023, *AJ*, 166, 50
 Humphreys, R. M., & McElroy, D. B. 1984, *ApJ*, 284, 565
 Hyland, A. R., Thomas, J. A., & Robinson, G. 1978, *AJ*, 83, 20
 Isserstedt, J. 1975, *A&AS*, 19, 259
 Isserstedt, J. 1979, *A&AS*, 38, 239
 Isserstedt, J. 1982, *A&AS*, 50, 7
 Jaschek, M. 1978, Catalog of Selected Spectral Types in the MK System (Strasbourg: Centre de Donnees Stellaires)
 Jaxon, E. G., Guerrero, M. A., Howk, J. C., et al. 2001, *PASP*, 113, 1130

- Kavanagh, P. J., Sasaki, M., & Points, S. D. 2012, *A&A*, **547**, A19
- Keenan, P. C., & McNeil, R. C. 1976, An Atlas of Spectra of the Cooler Stars: Types G,K,M,S, and C, Part 1: Introduction and Tables (Columbus, OH: Ohio State Univ. Press)
- Le Borgne, J. F., Bruzual, G., Pelló, R., et al. 2003, *A&A*, **402**, 433
- Levesque, E. M., Massey, P., Olsen, K. A. G., et al. 2006, *ApJ*, **645**, 1102
- Lundgren, K. 1988, *A&A*, **200**, 85
- Malumuth, E. M., & Heap, S. R. 1994, *AJ*, **107**, 1054
- Martayan, C., Frémat, Y., Hubert, A. M., et al. 2006, *A&A*, **452**, 273
- Martin, N., & Rebeirot, E. 1972, *A&A*, **21**, 329
- Martins, F., Schaerer, D., & Hillier, D. J. 2005, *A&A*, **436**, 1049
- Mason, B. D., Hartkopf, W. I., Gies, D. R., Henry, T. J., & Helsel, J. W. 2009, *AJ*, **137**, 3358
- Massey, P. 2002, *ApJS*, **141**, 81
- Massey, P., Lang, C. C., DeGioia-Eastwood, K., & Garmany, C. D. 1995, *ApJ*, **438**, 188
- Massey, P., Morrell, N. I., Neugent, K. F., et al. 2012, *ApJ*, **748**, 96
- Massey, P., Neugent, K. F., & Morrell, N. 2015, *ApJ*, **807**, 81
- Massey, P., Neugent, K. F., Morrell, N., & Hillier, D. J. 2014, *ApJ*, **788**, 83
- Massey, P., & Olsen, K. A. G. 2003, *AJ*, **126**, 2867
- Massey, P., Puls, J., Pauldrach, A. W. A., et al. 2005, *ApJ*, **627**, 477
- Massey, P., Waterhouse, E., & DeGioia-Eastwood, K. 2000, *AJ*, **119**, 2214
- McEvoy, C. M., Dufton, P. L., Evans, C. J., et al. 2015, *A&A*, **575**, A70
- McLeod, A. F., Dale, J. E., Evans, C. J., et al. 2019, *MNRAS*, **486**, 5263
- Melnick, J. 1985, *A&A*, **153**, 235
- Meynadier, F., Heydari-Malayeri, M., & Walborn, N. R. 2005, *A&A*, **436**, 117
- Morgan, D. H., Watson, F. G., & Parker, Q. A. 1992, *A&AS*, **93**, 495
- Mould, J., & Reid, N. 1987, *ApJ*, **321**, 156
- Neugent, K. F., Levesque, E. M., Massey, P., & Morrell, N. I. 2019, *ApJ*, **875**, 124
- Neugent, K. F., Levesque, E. M., Massey, P., Morrell, N. I., & Drout, M. R. 2020, *ApJ*, **900**, 118
- Neugent, K. F., Massey, P., & Morrell, N. 2018, *ApJ*, **863**, 181
- Neugent, K. F., Massey, P., Skiff, B., & Meynet, G. 2012, *ApJ*, **749**, 177
- Oestreich, M. O., Schmidt-Kaler, T., & Wargau, W. 1997, *MNRAS*, **289**, 729
- Oey, M. S. 1996a, *ApJS*, **104**, 71
- Oey, M. S. 1996b, *ApJ*, **465**, 231
- Oey, M. S., & Massey, P. 1995, *ApJ*, **452**, 210
- Parker, J. W. 1992, *PASP*, **104**, 1107
- Parker, J. W. 1993, *AJ*, **106**, 560
- Parker, J. W., & Garmany, C. D. 1993, *AJ*, **106**, 1471
- Parker, J. W., Garmany, C. D., Massey, P., & Walborn, N. R. 1992, *AJ*, **103**, 1205
- Parker, J. W., Zaritsky, D., Stecher, T. P., Harris, J., & Massey, P. 2001, *AJ*, **121**, 891
- Patrick, L. R., Lennon, D. J., Britavskiy, N., et al. 2019, *A&A*, **624**, A129
- Paul, K. T., Subramaniam, A., Mathew, B., Mennickent, R. E., & Sabogal, B. 2012, *MNRAS*, **421**, 3622
- Ramachandran, V., Hamann, W. R., Hainich, R., et al. 2018, *A&A*, **615**, A40
- Rebeirot, E., Martin, N., Mianes, P., et al. 1983, *A&AS*, **51**, 277
- Reid, N., & Mould, J. 1985, *ApJ*, **299**, 236
- Reid, N., Tinney, C., & Mould, J. 1990, *ApJ*, **348**, 98
- Reid, W. A., & Parker, Q. A. 2012, *MNRAS*, **425**, 355
- Ridley, J. P., Crawford, F., Lorimer, D. R., et al. 2013, *MNRAS*, **433**, 138
- Rivero González, J. G., Puls, J., Najarro, F., & Brott, I. 2012, *A&A*, **537**, A79
- Rousseau, J., Martin, N., Prévot, L., et al. 1978, *A&AS*, **31**, 243
- Sana, H. 2017, in IAU Symp. 329, The Lives and Death-Throes of Massive Stars, ed. J. J. Eldridge (Cambridge: Cambridge Univ. Press), 110
- Sana, H., de Koter, A., de Mink, S. E., et al. 2013, *A&A*, **550**, A107
- Sanduleak, N. 1970, *CoTol*, **89**, 1
- Sanduleak, N. 1972, *A&A*, **17**, 326
- Sanduleak, N., & Philip, A. G. D. 1977, *PW&SO*, **2**, 105
- Schild, H., & Testor, G. 1992, *A&AS*, **92**, 729
- Schmidt-Kaler, T., Gohermann, J., Oestreich, M. O., et al. 1999, *MNRAS*, **306**, 279
- Selier, R., & Heydari-Malayeri, M. 2012, *A&A*, **545**, A29
- Shanti Priya, D., Sriram, K., & Vivekananda Rao, P. 2011, *RAA*, **11**, 175
- Shore, S. N., & Sanduleak, N. 1984, *ApJS*, **55**, 1
- Smith Neubig, M. M., & Bruhwiler, F. C. 1999, *AJ*, **117**, 2856
- Stock, J., Osborn, W., & Ibáñez, M. 1976, *A&AS*, **24**, 35
- Testor, G., & Niemela, V. 1998, *A&AS*, **130**, 527
- Thompson, G. I., Nandy, K., Morgan, D. H., et al. 1982, *MNRAS*, **200**, 551
- van Jaarsveld, N., Buckley, D. A. H., McBride, V. A., et al. 2018, *MNRAS*, **475**, 3253
- Wagner-Kaiser, R., Mackey, D., Sarajedini, A., et al. 2017, *MNRAS*, **471**, 3347
- Walborn, N. R. 1977, *ApJ*, **215**, 53
- Walborn, N. R., & Blades, J. C. 1997, *ApJS*, **112**, 457
- Walborn, N. R., Fullerton, A. W., Crowther, P. A., et al. 2002a, *ApJS*, **141**, 443
- Walborn, N. R., Howarth, I. D., Evans, C. J., et al. 2010, *AJ*, **139**, 1283
- Walborn, N. R., Maíz-Apellániz, J., & Barbá, R. H. 2002b, *AJ*, **124**, 1601
- Walborn, N. R., Sana, H., Simón-Díaz, S., et al. 2014, *A&A*, **564**, A40
- Weidner, C., & Vink, J. S. 2010, *A&A*, **524**, A98
- Wenger, M., Ochsenbein, F., Egret, D., et al. 2000, *A&AS*, **143**, 9
- Westerlund, B. E., Olander, N., & Hedin, B. 1981, *A&AS*, **43**, 267
- Will, J. M., Bomans, D. J., & Dieball, A. 1997, *A&AS*, **123**, 455
- Wood, P. R., Bessell, M. S., & Fox, M. W. 1983, *ApJ*, **272**, 99
- Zacharias, N., Finch, C. T., Girard, T. M., et al. 2012, *AJ*, **145**, 44
- Zaritsky, D., Harris, J., Thompson, I. B., & Grebel, E. K. 2004, *AJ*, **128**, 1606
- Zastrow, J., Oey, M. S., & Pellegrini, E. W. 2013, *ApJ*, **769**, 94
- Zickgraf, F. J., Wolf, B., Stahl, O., Leitherer, C., & Appenzeller, I. 1986, *A&A*, **163**, 119